energies

MDPI

Article

Size-Dispersed Calcium Phosphate-Based Paints for Sustainable, Durable Cool Roof Applications

Andrew Caratenuto [1,2], Sunny Leung [2], Nathaniel LeCompte [2] and Yi Zheng [1,2,3,*]

[1] Department of Mechanical and Industrial Engineering, Northeastern University, Boston, MA 02115, USA
[2] Planck Energies Inc., Boston, MA 02135, USA
[3] Department of Chemical Engineering, Northeastern University, Boston, MA 02115, USA
* Correspondence: y.zheng@northeastern.edu

Abstract: Passive radiative cooling materials are widely recognized as attractive innovations for reducing emissions and expanding life-saving cooling access. Despite immense research attention, the adoption of such technologies is limited largely due to a lack of scalability and cost compatibility with market needs. While paint and coating-based approaches offer a more sensible solution, many demonstrations suffer from issues such as a low solar reflectance performance or a lack of material sustainability due to the use of harmful solvents. In this work, we demonstrate a passive radiative cooling paint which achieves an extremely high solar reflectance value of 98% using a completely water-based formulation. Material sustainability is promoted by incorporating size-dispersed calcium phosphate biomaterials, which offer broadband solar reflectance, as well as a self-crosslinking water-based binder, providing water resistance and durability without introducing harmful materials. Common industry pigments are integrated within the binder for comparison, illustrating the benefit of finely-tuned particle size distributions for broadband solar reflectance, even in low-refractive-index materials such as calcium phosphates. With scalability, outdoor durability, and eco-friendly materials, this demonstrated paint offers a practical passive radiative cooling approach without exacerbating other environmental issues.

Keywords: calcium phosphate; solar reflectance; cool roof; paint; sustainability

Citation: Caratenuto, A.; Leung, S.; LeCompte, N.; Zheng, Y. Size-Dispersed Calcium Phosphate-Based Paints for Sustainable, Durable Cool Roof Applications. *Energies* **2024**, *17*, 4178. https://doi.org/10.3390/en17164178

Academic Editor: F. Pacheco Torgal

Received: 10 July 2024
Revised: 15 August 2024
Accepted: 20 August 2024
Published: 22 August 2024

1. Introduction

A great variety of functional passive radiative cooling (PRC) materials have been demonstrated, presenting great opportunities for reducing carbon emissions and heat-related illnesses and deaths across the globe. This potential is particularly relevant for low-income and vulnerable populations who stand to benefit greatly from such technologies [1–5]. However, not all demonstrated techniques are practical for actual applications on infrastructure. Perhaps the most promising and impactful use case for PRC is on buildings. Buildings consume massive amounts of energy to maintain comfortable internal conditions, representing one of the most significant contributions to global energy consumption [6]. Further, building roofing and facades cover a vast area in nearly every country, offering a substantial market for PRC products [7,8]. However, such applications demand other attributes besides cooling ability alone. Roof coatings, for example, are designed largely for the purpose of protecting the structure and sealing off the internal environment from the elements. These coatings must be cost-competitive, as consumers tend to prioritize lower-priced roof coating solutions. Durability is also a paramount concern, with most existing roof coatings targeting longevity of a decade or longer. Simultaneously, ease of installation should be maximized to guarantee a wide acceptance of the solution and encourage adoption [9–11].

The most obvious PRC approach that supports all of these requirements is a paint-like solution. Paints and coatings are widely used on buildings and many other industries owing

to their versatility, relatively low cost, and durability. As such, many incumbent roof coating products are applied using paint-like approaches [9–11]. PRC research in recent years has concentrated heavily on paint-based solutions as well, largely due to the aforementioned benefits [1,6,12–17]. Yet, despite the inherent environmental consciousness of the PRC approach, many demonstrated paints in the recent literature utilize harmful materials. Hazardous solvents comprising VOCs and formaldehydes are common [6,16,17], as well as reliance upon pigments and additives that present environmental issues [13,18]. A truly sustainable PRC paint must not only exhibit highly efficient radiative cooling properties, but must also comprise eco-friendly and non-toxic materials. Furthermore, it is also of paramount importance for such paints to maintain durability, cost-effectiveness, and ease of application in line with existing roof coating products to better support market adoption.

To help address these points, a PRC paint with superior cooling, industry-relevant multifunctionalities, and overall sustainability was designed and evaluated within this study (Figure 1). The synthesis of this paint requires no VOCs or harmful solvents and utilizes only calcium-based biomaterials as pigments and fillers. Despite the fully water-based formulation, the dried paint exhibits a high water resistance and durability, providing feasibility for the outdoor application demanded of PRC materials. Along with simple synthesis and application, these attributes provide the demonstrated calcium-based PRC paint with both the sustainability and performance features required for widespread adoption.

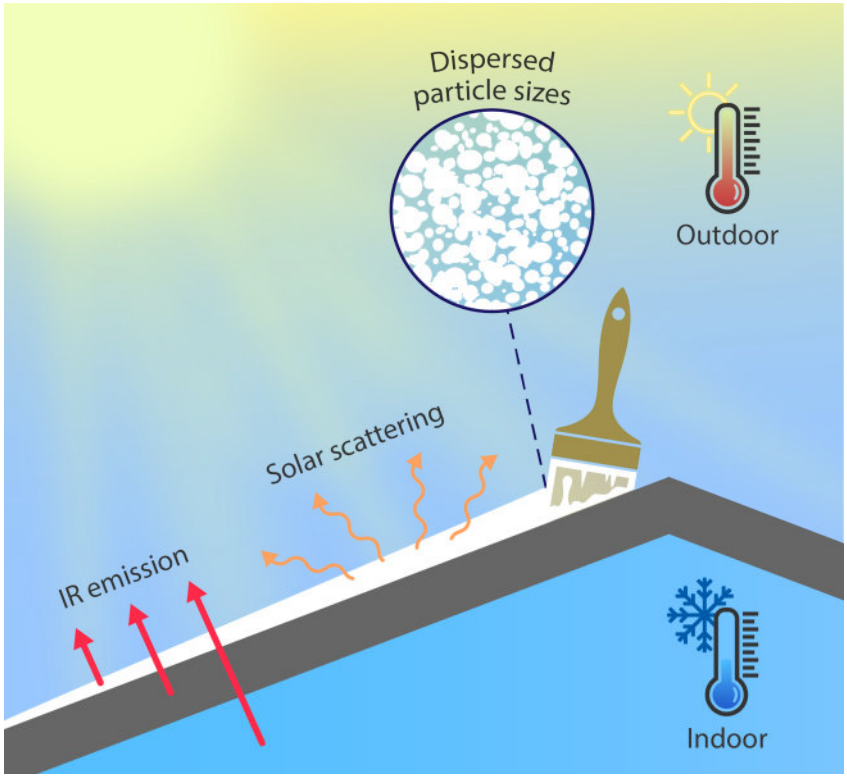

Figure 1. Schematic representation of passive radiative cooling paint. The CaP-based paint exemplified in this work possesses a dispersed range of pigment particle sizes, which enable broadband scattering of incident solar radiation.

2. Materials and Methods

2.1. Materials

Calcium nitrate tetrahydrate (CAS 13477-34-4), calcium carbonate (CAS 471-34-1), and ammonium phosphate dibasic (CAS 7783-28-0) were purchased from Sigma-Aldrich (St. Louis, MO, USA). Ottopol SF-49 was obtained from Gellner Industrial (Tamaqua, PA, USA). Titanium dioxide (Ti-Pure R-706) was obtained from Chemours (Wilmington, DE, USA). Disperbyk-2010 was obtained from BYK (Wesel, Germany), and Farm General

Defoamer was obtained from Ragan & Massey LLC (Ponchatoula, LA, USA). The commercial paint used for abrasion testing comparison was obtained from Rust-Oleum (Mount Waverley, VIC, Australia) (Semi-gloss White, Ultra Cover Premium Latex Paint).

2.2. Synthesis

2.2.1. Calcium Pyrophosphate Pigment

To synthesize the CPP pigment, a Ca/P ratio of 1.0 was used. First, 28.35 g calcium nitrate tetrahydrate ($Ca(NO_3)_2$) was added to 400 mL DI water. Then, 15.84 g ammonium phosphate dibasic ($(NH_4)_2HPO_4$) was also added to 400 mL DI water. Beakers were brought to a temperature of 60 °C while stirring and then stirred for an additional 30 min. Afterwards, the ammonium hydrogen phosphate solution was added to the calcium nitrate solution while stirring the latter solution. The addition rate of the ammonium hydrogen phosphate solution was about 25 mL min^{-1}. Then, the combined solution was stirred for an additional 90 min without heating. The solution was then rested overnight. After resting, the product was vacuum-filtered using a Grade 4 filter paper and rinsed with DI water. The filtered precipitate was dried at 60 °C overnight and then ground using a mechanical grinder. Then, the powder was calcined for 1 h at 700 °C to obtain the finalized CPP pigment.

2.2.2. PRC Paint

First, the CPP pigment was ground once more in a mechanical grinder followed by crushing to a fine particle size using an agate mortar and pestle. DI water (10 mL), Ottopol SF-49 (10 mL), Disperbyk-2010 (0.25 mL), and defoamer (0.50 mL) were combined and stirred briefly by hand. Then, 4 g of ground CPP was added to the solution in small increments, stirring each time until combined. Once all CPP was added, the paint mixture was mixed using a FSH-2B high-speed homogenizer at approximately 10,000 rpm for 2 min. The paint was then placed in an ultrasonicator for 10 min. Finally, the paint was poured onto a plastic substrate with an approximate thickness of 0.5 mm and left to dry for 24 h. The same procedure was used for the $CaCO_3$ and TiO_2 paints, replacing the CPP pigment with equal masses of the alternative materials. The pure Ottopol sample was simply poured in a dish without further modification (thickness 1.4 mm) and left to dry for 24 h.

2.3. Characterization

Reflectance spectra in the UV/visible/NIR region were characterized using the Jasco V770 using the ISN-923 integrating sphere (incidence angle of 6°). A Spectralon SRS-99-010 diffuse reflectance standard was used to calibrate and correct UV/visible/NIR spectra to obtain absolute reflectance. Reflectance spectra in the IR region were characterized using the Jasco FTIR 6600 equipped with a PIKE integrating sphere (incidence angle of 12°). Scanning electron microscopy (SEM) images were obtained using the Supra 25 SEM at an acceleration voltage of 5 kV. A gold/palladium surface coating of about 10 nm was deposited on SEM samples for imaging. Contact angles were obtained using the SINDIN SDC-350 contact angle meter. The adhesion test was modeled after ASTM D3359. The paint sample was cut with a razor, and a strip of tape was pressed onto the paint surface using a 1 kg mass. After pressing, the tape was removed and inspected for residue. Water resistance was studied by placing the samples in a large beaker of DI water stirred at 350 RPM for 1 h. The surfaces were assessed visually, and spectral performance before and after exposure to water was measured. After the water exposure test, the same sample was subsequently exposed to UV radiation for 5 days under an irradiance of 5 mW cm^{-2} using a UVBeast V1 flashlight. Abrasion tests were performed using a Taber type abraser (Roweel Electronic Co., Ltd., Zhengzhou, China) using CS-10 abrasion wheels (Elcometer, Manchester, UK) with masses of 250 g. The wheels were resurfaced every 500 cycles. Resurfacing was performed with 25 cycles of S-11 resurfacing disks. Rust-Oleum Semi-gloss White was used as the commercial paint comparison.

3. Results and Discussion

3.1. Optical Performance

PRC materials provide cooling without electricity based on their finely tuned optical properties. Firstly, they must minimize the energy absorbed from the sun by reflecting as much incident solar irradiation (0.3–2.5 µm) as possible. In addition, they must also maximize the radiative energy output in the mid-IR region, where objects at typical terrestrial temperatures emit radiation. IR emittance may also be optimized by focusing on the atmospheric transparency window (8–13 µm). In this region, sky-facing surfaces may emit without receiving large amounts of radiation back from the Earth's atmosphere, allowing for a greater net transfer of energy from the surface [1,19]. Together, a high solar reflectance and strong IR emittance limit energy input and maximize energy output, allowing for PRC materials to passively cool. Hence, these optical properties are the major focus in the development and characterization of PRC materials.

The main pigment utilized in the PRC paints for this study was calcium pyrophosphate (CPP). In addition, $CaCO_3$ and TiO_2 were used as comparison groups, as these materials are utilized commonly as fillers and pigments, respectively, throughout the paint industry [1]. The morphology of the paint surfaces as well as that of each pigment can be seen in Figure 2. The top surfaces of all paints appear fairly flat and greatly resemble that of the unfilled Ottopol binder (Figure 3). This indicates that most of the pigment is encapsulated within the binder rather than protruding out of the top surface.

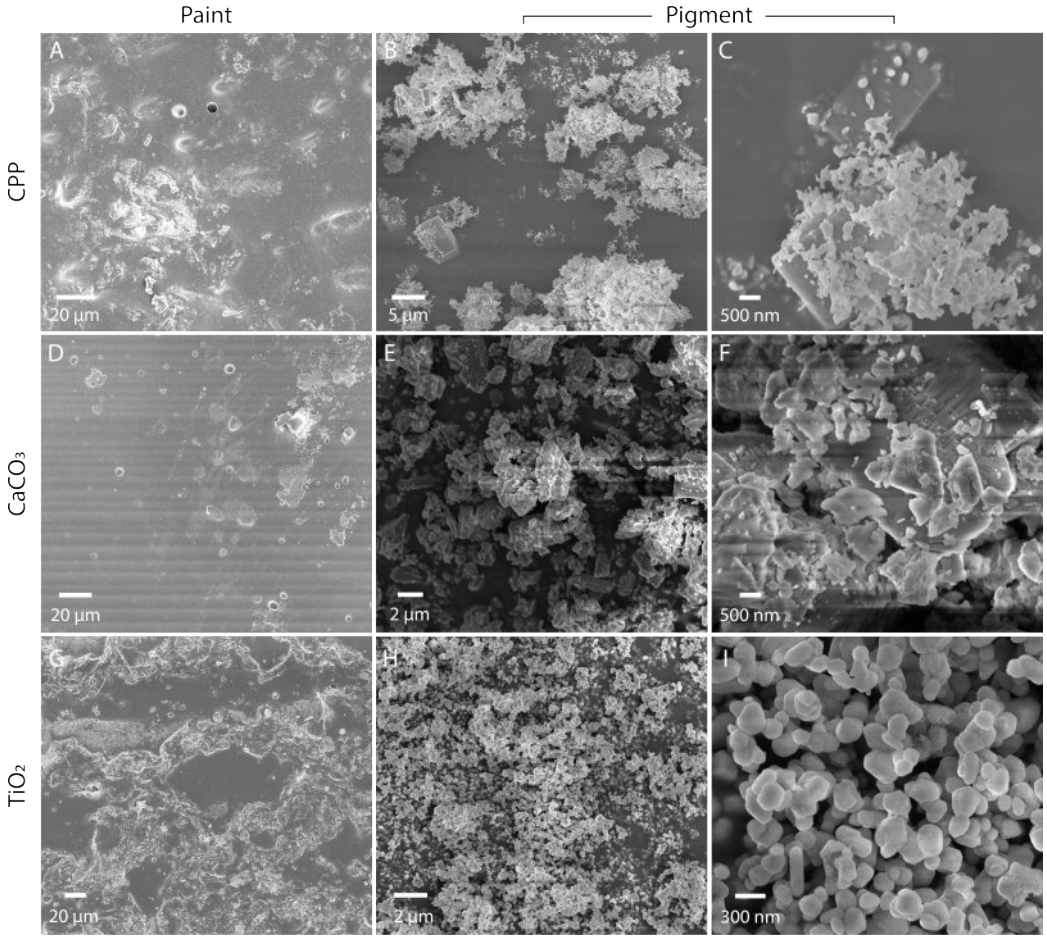

Figure 2. SEM images. (**A**) CPP paint top surface and (**B**,**C**) CPP pigment. (**D**) $CaCO_3$ paint top surface and (**E**,**F**) $CaCO_3$ pigment. (**G**) TiO_2 paint top surface and (**H**,**I**) TiO_2 pigment.

Both the CPP and $CaCO_3$ pigments show a fairly broad particle size distribution. The CPP in particular has feature sizes as large as 5 µm and as small as several hundred

nanometers. The feature sizes of the $CaCO_3$ fall in approximately the same range, though there appears to be a greater bias towards larger particles in the case of the $CaCO_3$. In contrast, the TiO_2 particles have a much tighter range of feature sizes, ranging from about 150 nm to slightly over 300 nm. No larger micron-scale structures are present, in line with the mean particle size of 360 nm specified by the manufacturer. These morphological features have a strong influence on the PRC performance of the paints, as discussed in subsequent sections.

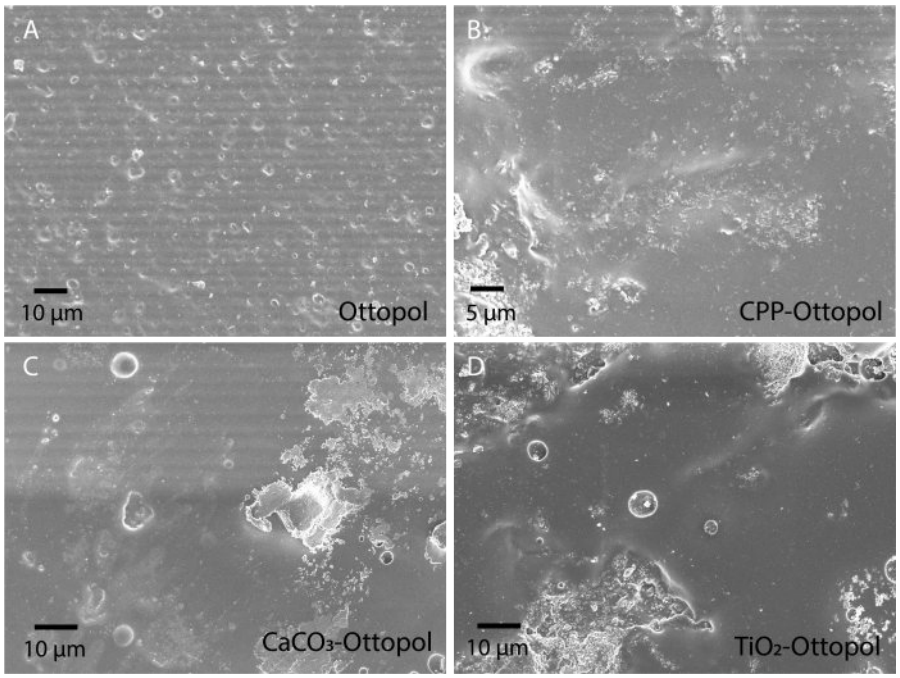

Figure 3. SEM images of unfilled Ottopol binder and paint samples. (**A**) Unfilled Ottopol binder, (**B**) CPP paint, (**C**) $CaCO_3$ paint, and (**D**) TiO_2 paint under SEM.

The spectral reflectance of all paint samples are shown in Figure 4. The binder itself (Ottopol) exhibits low reflectance and high transmittance when unfilled. When filled with the various pigment materials, the synthesized paints show a very high reflectance throughout most of the solar wavelength region, leading to normalized solar reflectance values from 92% to nearly 99%. The near-IR for all paints shows absorbance bands that coincide with those of the unfilled Ottopol, indicating that these are due to absorbance by the binder. However, these absorbance peaks are diminished in the filled paints, as the penetration depth is limited by particle scattering, leading to a higher reflectance.

One notable characteristic of the TiO_2-based paint is its comparatively low reflectance at short visible and UV wavelengths. This is expected based on intrinsic properties of TiO_2. Its high refractive index provides strong opacity when used within acrylic paint media, as the high refractive index differential between the matrix and pigment greatly supports scattering. Yet, one drawback of its high refractive index is unavoidable absorption losses at lower wavelengths, due to its relatively small bandgap [1,20]. CPP and $CaCO_3$ have lower refractive indices, which often makes their scattering performance fall below that of TiO_2—especially when used at a relatively low volume concentration (i.e., less than 10%) within paint formulations. However, lower-index materials benefit from less optical absorption at shorter wavelengths due to their larger band gaps [20], often providing stronger scattering in the UV and short visible regions, as is seen in Figure 4A. In addition, the pigment volume concentration utilized here is relatively high—about 16% to 26%, dependent upon material density. In combination with the aforementioned factors, this provides both the CPP and $CaCO_3$ paints with higher overall reflectance performance in comparison to the TiO_2.

The reflectance values of paints in the IR region are very similar. All paints share an IR emittance of approximately 0.92 when normalized to a 20 °C blackbody (Figure 4B). Although the spectra diverge at lower IR wavelengths (2.5–5 µm), the blackbody spectra for common terrestrial temperatures is biased towards wavelengths of 8 µm and larger. All spectra are very consistent within this latter region, leading to their similarity in normalized emittance values. The high emittance in the mid-IR region is attributed mainly to the acrylic-based paint matrix. This is verified by the reflectance spectra of the unfilled binder, which closely matches that of all paints throughout most of the IR region. Organic polymers typically possess strong emittance within this region due to the optical phonon modes of many common monomer groups, making most paints and coatings act as strong IR emitters without requiring additional treatment [15,21].

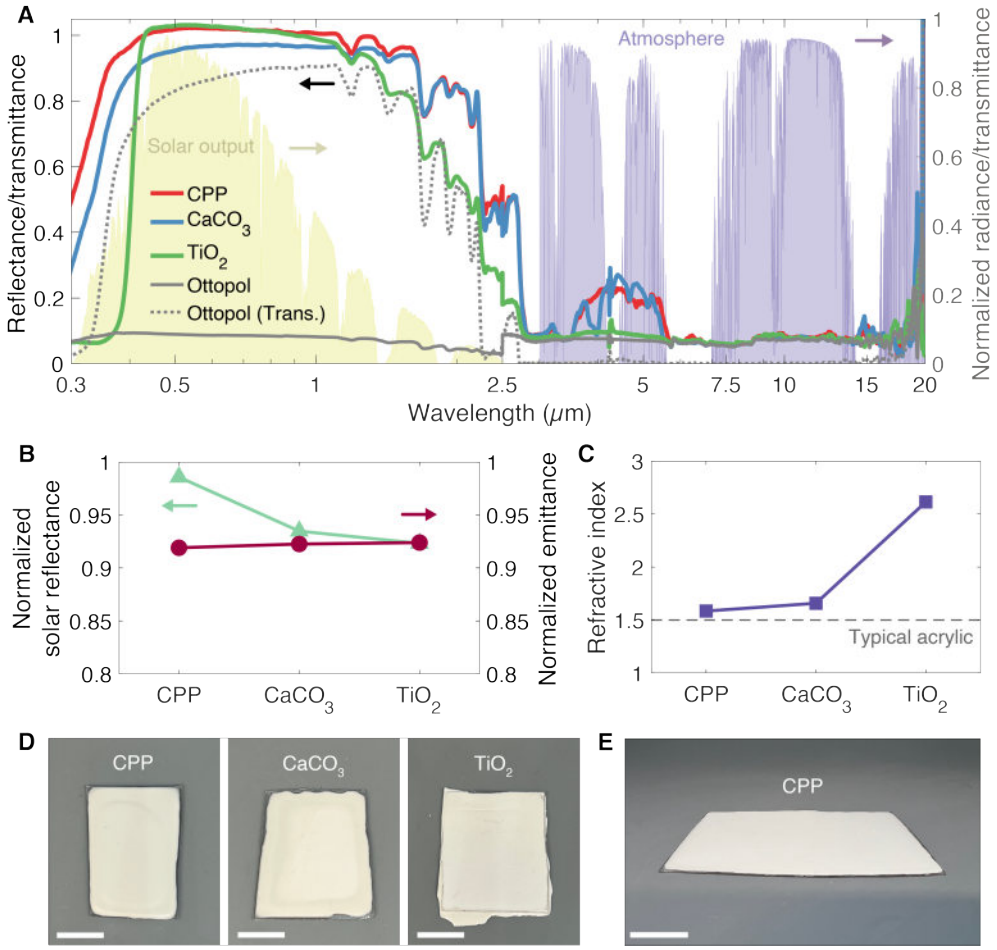

Figure 4. Spectral performance of PRC paints. (**A**) Spectral reflectance of paint samples from 0.3 to 20 µm (left axis). AM 1.5 solar irradiance [22] and atmospheric transmittance [23] are shown for comparison (right axis). (**B**) Normalized solar reflectance (left axis) and IR emittance (right axis). Solar reflectance is normalized based on the AM 1.5 irradiance spectrum, and IR emittance is normalized based on a blackbody at 20 °C. (**C**) Refractive indices of pigment materials in the visible region. (**D**) Images of paint samples on plastic substrates. Scale bar is approximately 1 cm. (**E**) Demonstration of application scalability of CPP-based paint. Scale bar is approximately 2 cm.

The CPP and $CaCO_3$ paints show notable similarities, both in reflectance magnitude and spectral features. Yet, one may expect them to be even more similar, especially on the basis of normalized solar reflectance, based on their closeness in refractive index and density. We attribute the greater performance of the CPP paint to the CPP pigment possessing a more favorable particle size distribution for scattering solar radiation. A distributed range of particle sizes—generally in the mid-nanometer to low-micron range—has been

shown to be instrumental for broadband solar reflectance [24]. While both raw materials possess a similar range of feature sizes (as seen in the SEM images), the CPP pigment does exhibit a higher proportion of smaller particle sizes than the $CaCO_3$. Smaller particles are generally more effective at scattering smaller wavelengths, as exemplified previously [24]. Consequently, the CPP paint exhibits a higher reflectance at shorter wavelengths as expected. Simultaneously, the presence of larger particle sizes still allow it to maintain high reflectance at longer wavelengths as well, contributing to its extremely high normalized reflectance value.

The case of the TiO_2 paint provides another illustration of the impact of morphology. TiO_2 feature sizes around 300 nm are particularly suitable for reflecting visible light, leading to their widespread use in the industry as a white pigment. While this chosen particle size provides a visually bright white color, it also limits reflectance performance at longer wavelengths. The lack of large particle sizes in the TiO_2 paint is directly responsible for the low near-IR reflectance exhibited by this sample, leading to its lowered normalized reflectance. This provides a direct demonstration of the importance of broad particle size distributions in PRC paints.

3.2. Durability

In addition to optical performance, the durability of the paints is assessed to illustrate their suitability for long-term outdoor environmental use, as shown in Figure 5. First and foremost, the influence of water on the paints is studied. Both unfilled and filled paints show a relatively high water contact angle, which slowly diminishes over time. While this material is, therefore, not superhydrophobic like other demonstrated PRC materials [25], the larger contact angle will support resistance to contamination buildup. The paints themselves exhibit extremely strong resistance to intense contact with water. As seen in Figure 5C, both pre-marred and pristine CPP paint samples appear unaffected by water exposure after stirring in water at 350 RPM for 1 h. After the water exposure test, the same sample is subsequently exposed to UV radiation using a UV flashlight (Figure 5D) for 5 days. As shown in Figure 5E, neither intense water exposure nor constant UV irradiance affect the spectral performance of the CPP paint. This indicates that the CPP paint is a great candidate for applications in outdoor environments, as its resistance to degradation in rain and constant sunlight exposure will extend its lifetime.

In addition, the mechanical strength of the paints is demonstrated using a variety of methods. First, a simple bending evaluation is performed to test the resistance of the coating to deformation-induced cracking. The CPP paint, on an acrylic substrate, is bent by hand to an angle of approximately 90°, as shown in Figure 6A. Both upward and downward bends were repeated for 50 cycles, after which the coating was visually inspected. As seen in Figure 6A, there are no signs of cracking or other damage, indicating that the CPP paint exhibits strong flexibility and mechanical stability. This bodes well for outdoor applications, where structures may experience thermal expansion or other types of deformation due to weather conditions, seasonal variation, or human activity. Therefore, practical PRC coatings must be able to withstand such variations to remain stable over long periods of time. Adhesion is also demonstrated by performing a tape test, shown in Figure 6B. After cross-cutting the CPP paint sample and pressing tape onto the surface with a 1 kg mass, barely any residue is seen on the surface of the paint. This is comparable to the result exhibited by a commercial paint in a previous demonstration [19]. Finally, the resistance of the PRC coating to abrasion is characterized. As seen in Figure 6C, the CPP paint shows similar resistance to abrasion as compared with a commercial latex paint. The total mass loss after 1500 abrasion cycles is about 27% higher in the CPP paint than the commercial paint, thus exhibiting a similar order of magnitude in wear resistance. These durability results illustrate that the demonstrated PRC paints based on CPP and the Ottopol binder exhibit fantastic characteristics for practical applications, not only in terms of spectral performance, but also on the basis of durability in harsh environments.

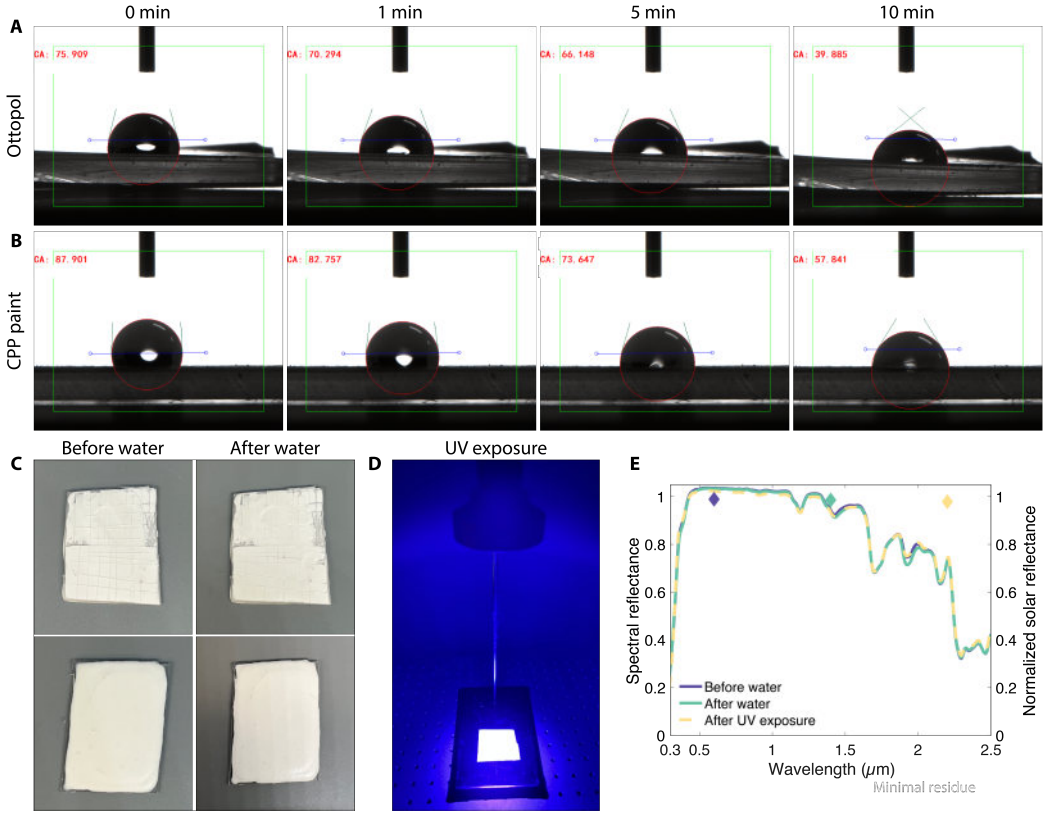

Figure 5. Water and UV resistance. Contact angles of (**A**) Ottopol binder film without pigment and (**B**) CPP paint over time. (**C**) Marred (top) and pristine (bottom) CPP paint samples before and after spinning in water for 1 h at 350 RPM. No signs of wear or degradation are notable. (**D**) CPP paint under exposure of UV radiation. (**E**) Spectral and normalized reflectance of CPP paint samples in response to intense water exposure (1 h at 350 RPM) and subsequent UV exposure (5 days at 5 mW cm^{-2}).

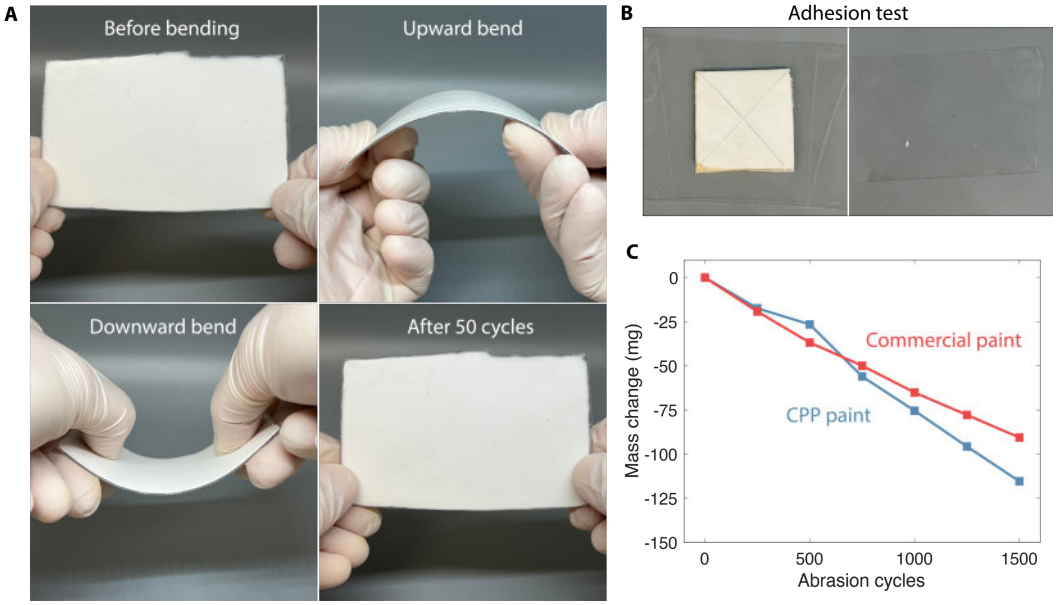

Figure 6. Mechanical durability. (**A**) Bending evaluation of CPP paint on acrylic substrate. No cracking is visible after 50 cycles of upwards and downwards bending to approximately 90°. (**B**) Tape adhesion test results of CPP, showing minimal residue after the tape is removed. (**C**) Abrasion test results of Ottopol-CPP paint versus a commercial latex paint.

4. Conclusions

In this work, a paint-focused approach to PRC is demonstrated using all-natural materials. A water-based binder is used to encapsulate various solar-reflective pigments to achieve high solar reflectance for cool-roof applications. While all demonstrated paints achieve relatively high reflectance, the calcium pyrophosphate paint exhibits the strongest performance, providing a near-ideal broadband solar reflectance of 98%. In addition, the polymeric binder provides a strong mid-IR emittance of 92% for all evaluated paints. An investigation of the morphology of constituent materials reveals that the dispersed range of particle sizes possessed by the calcium pyrophosphate pigment—from several hundred nanometers to the low-micron range—lead to its notable PRC performance features. Finally, the water resistance, durability, and adhesion of the synthesized paints are demonstrated, including a lack of optical performance loss after prolonged water and UV exposure. These factors provide evidence of the suitability of the PRC paint for real outdoor applications. Due to its balance of optical performance and practicality, this simple, eco-friendly paint-based PRC approach has great potential for emission reduction and thermal comfort enhancement worldwide.

Author Contributions: Conceptualization, A.C., N.L. and Y.Z.; Methodology, A.C., S.L. and Y.Z.; Software, A.C.; Validation, S.L.; Formal analysis, A.C.; Investigation, S.L. and N.L.; Resources, Y.Z.; Writing—original draft preparation, A.C.; Writing—review and editing, S.L., N.L. and Y.Z.; Visualization, A.C.; Supervision, A.C. and Y.Z.; Project administration, Y.Z.; Funding acquisition, Y.Z. All authors have read and agreed to the published version of the manuscript.

Funding: This work is supported by NSF CBET-1941743 and NSF TI-2321446.

Data Availability Statement: The data that support the findings of this study are available from the corresponding author upon reasonable request.

Conflicts of Interest: Authors Andrew Caratenuto, Sunny Leung, Nathaniel LeCompte and Yi Zheng were employed by the company Planck Energies Inc.

References

1. Mandal, J.; Yang, Y.; Yu, N.; Raman, A.P. Paints as a Scalable and Effective Radiative Cooling Technology for Buildings. *Joule* **2020**, *4*, 1350–1356. [CrossRef]
2. Anderson, G.B.; Bell, M.L. Heat Waves in the United States: Mortality Risk during Heat Waves and Effect Modification by Heat Wave Characteristics in 43 U.S. Communities. *Environ. Health Perspect.* **2011**, *119*, 210–218. [CrossRef] [PubMed]
3. Santamouris, M.; Pavlou, K.; Synnefa, A.; Niachou, K.; Kolokotsa, D. Recent progress on passive cooling techniques: Advanced technological developments to improve survivability levels in low-income households. *Energy Build.* **2007**, *39*, 859–866. [CrossRef]
4. Santamouris, M.; Khan, H.S.; Paolini, R.; Julia, O.M.L.; Garshasbi, S.; Papakonstantinou, I.; Valenta, J. Recent Advances in Fluorescence-Based Colored Passive Daytime Radiative Cooling for Heat Mitigation. *Int. J. Thermophys.* **2024**, *45*, 90. [CrossRef]
5. Morales-Inzunza, S.; González-Trevizo, M.E.; Martínez-Torres, K.E.; Luna-León, A.; Tamayo-Pérez, U.J.; Fernández-Melchor, F.; Santamouris, M. On the potential of cool materials in the urban heat island context: Scalability challenges and technological setbacks towards building decarbonization. *Energy Build.* **2023**, *296*, 113330. [CrossRef]
6. Li, X.; Peoples, J.; Huang, Z.; Zhao, Z.; Qiu, J.; Ruan, X. Full Daytime Sub-ambient Radiative Cooling in Commercial-like Paints with High Figure of Merit. *Cell Rep. Phys. Sci.* **2020**, *1*, 100221. [CrossRef]
7. Gagnon, P.; Margolis, R.; Melius, J.; Phillips, C.; Elmore, R. *Rooftop Solar Photovoltaic Technical Potential in the United States. A Detailed Assessment*; Technical Report NREL/TP–6A20-65298; National Renewable Energy Laboratory: Golden, CO, USA, 2016; p. 1236153. [CrossRef]
8. Joshi, S.; Mittal, S.; Holloway, P.; Shukla, P.R.; Ó Gallachóir, B.; Glynn, J. High resolution global spatiotemporal assessment of rooftop solar photovoltaics potential for renewable electricity generation. *Nat. Commun.* **2021**, *12*, 5738. [CrossRef] [PubMed]
9. Levin, J.R.; Daisey, G.; Elbert, K.C.; Mallardi, J.; Westmeyer, M.; Williams, D. Acrylic Binder and Formulation Design for More Sustainable Elastomeric Cool Roof Coatings (ERCs). In *ACS Symposium Series*; Cheng, H.N., Gross, R.A., Eds.; American Chemical Society: Washington, DC, USA, 2023; Volume 1451, pp. 203–218. [CrossRef]
10. Muruzina, E.V.; Murzagalina, E.I. Study of the eco-friendly roofing materials based on elastomers in accelerated modes. *Procedia Environ. Sci. Eng. Manag.* **2020**, *7*, 571–579.
11. Pisello, A.L. State of the art on the development of cool coatings for buildings and cities. *Sol. Energy* **2017**, *144*, 660–680. [CrossRef]
12. Gong, Q.; Lu, L.; Chen, J.; Yin Lau, W.; Ho Cheung, K. A novel aqueous scalable eco-friendly paint for passive daytime radiative cooling in sub-tropical climates. *Sol. Energy* **2023**, *255*, 236–242. [CrossRef]

13. Zhao, B.; Xu, C.; Jin, C.; Lu, K.; Chen, K.; Li, X.; Li, L.; Pei, G. Superhydrophobic bilayer coating for passive daytime radiative cooling. *Nanophotonics* **2024**, *13*, 583–591. [CrossRef]
14. Sun, J.; Wang, J.; Guo, T.; Bao, H.; Bai, S. Daytime passive radiative cooling materials based on disordered media: A review. *Sol. Energy Mater. Sol. Cells* **2022**, *236*, 111492. [CrossRef]
15. Peoples, J.; Ruan, X. *Radiative Cooling Paints*; Elsevier: Amsterdam, The Netherlands, 2023; pp. 393–419.
16. Li, X.; Peoples, J.; Yao, P.; Ruan, X. Ultrawhite BaSO4 Paints and Films for Remarkable Daytime Subambient Radiative Cooling. *ACS Appl. Mater. Interfaces* **2021**, *13*, 21733–21739. [CrossRef]
17. Lv, J.; Chen, Z.; Li, X. Calcium Phosphate Paints for Full-Daytime Subambient Radiative Cooling. *ACS Appl. Energy Mater.* **2022**, *5*, 4117–4124. [CrossRef]
18. Kralikova, R.; Pinosova, M.; Koblasa, F.; Wessely, E.; Rusko, M. Environmental and Health Impact of Paint Products. In *DAAAM Proceedings*, 1st ed.; Katalinic, B., Ed.; DAAAM International: Vienna, Austria, 2020; Volume 1, pp. 35–43. [CrossRef]
19. Caratenuto, A.; Leach, K.; Liu, Y.; Zheng, Y. Nanofibrous Biomaterial-Based Passive Cooling Paint Structurally Linked by Alkane-Oleate Interactions. *ACS Appl. Mater. Interfaces* **2024**, *16*, 12717–12730. [CrossRef] [PubMed]
20. Tong, Z.; Peoples, J.; Li, X.; Yang, X.; Bao, H.; Ruan, X. Electronic and phononic origins of BaSO4 as an ultra-efficient radiative cooling paint pigment. *Mater. Today Phys.* **2022**, *24*, 100658. [CrossRef]
21. Incropera, F.P.; DeWitt, D.P.; Bergman, T.L.; Lavine, A.S. *Fundamentals of Heat and Mass Transfer*, 6th ed.; Wiley: Hoboken, NJ, USA, 2007.
22. NREL. Reference Air Mass 1.5 Spectra. Available online: https://www.nrel.gov/grid/solar-resource/spectra-am1.5.html (accessed on 30 June 2023).
23. SPIE. *MODTRAN4 Radiative Transfer Modeling for Atmospheric Correction*; Spectral Sciences, Inc.: Burlington, MA, USA, 1999; Volume 3756.
24. Peoples, J.; Li, X.; Lv, Y.; Qiu, J.; Huang, Z.; Ruan, X. A strategy of hierarchical particle sizes in nanoparticle composite for enhancing solar reflection. *Int. J. Heat Mass Transf.* **2019**, *131*, 487–494. [CrossRef]
25. Tian, Y.; Shao, H.; Liu, X.; Chen, F.; Li, Y.; Tang, C.; Zheng, Y. Superhydrophobic and recyclable cellulose-fiber-based composites for high-efficiency passive radiative cooling. *ACS Appl. Mater. Interfaces* **2021**, *13*, 22521–22530. [CrossRef] [PubMed]